ISSN 1063-7745, Crystallography Reports, 2019, Vol. 64, No. 5, pp. 793–797. © Pleiades Publishing, Inc., 2019.
Russian Text © The Author(s), 2019, published in Kristallografiya, 2019, Vol. 64, No. 5, pp. 776–780.

Comparison of Transmission Electron Microscopy and X-Ray Reflectometry Data in the Study of the Structure of Silicon-Carbon Nanocomposite Films

V. E. Asadchikov[a, b], Y. O. Volkov[a], I. G. Dyachkova[a], O. M. Zhigalina[a,c], V. M. Kanevsky[a], A. E. Muslimov[a], A. D. Nuzhdin[a], S. M. Pimenov[d], B. S. Roshchin[a,*], A. A. Rusakov[a], D. N. Khmelenin[a], S. Y. Shahbazov[e], and M. L. Shupegin[f]

[a] *Shubnikov Institute of Crystallography, Federal Research Center "Crystallography and Photonics," Russian Academy of Sciences, Moscow, 119333 Russia*

[b] *Moscow State University, Moscow, 119991 Russia*

[c] *Bauman Moscow State Technical University, Moscow, 105005 Russia*

[d] *Prokhorov General Physics Institute of the Russian Academy of Sciences, Moscow, 119991 Russia*

[e] *Research Institute of Advanced Materials and Technologies, Moscow, 105187 Russia*

[f] *National Research University "Moscow Power Engineering Institute," Moscow, 111250 Russia*

**e-mail: ross@crys.ras.ru*

Received February 6, 2019; revised February 6, 2019; accepted March 12, 2019

Abstract—Vanadium-doped diamond-like silicon-carbon films have been studied by X-ray reflectometry and transmission electron microscopy. A comparison of the data obtained has shown that the layered structure of the films is retained over an area of about 100 mm^2 at a total film thickness of 3–4 μm and layer thicknesses of 10–40 nm. The film surface has been examined by semi-contact probe microscopy. It is demonstrated that the root-mean-square roughness decreases by an order of magnitude (from 2.0 to 0.2 nm) with an increase in the vanadium content in the film from 12 to 17 at %.

DOI: 10.1134/S1063774519050031

INTRODUCTION

In recent years, films of nanocomposites based on a silicon-carbon matrix from plasma-polymerized polymethylphenylsiloxane (PMPS) and a metal carbide nanophase have attracted increasing attention both in Russia and abroad [1, 2]. The well-established name *diamond-like nanocomposite* (DLN) [3] is associated with the high concentration of sp^3 bonds between carbon atoms in the film structure. The increased interest in these materials is due to their high resistance against aggressive media. We should note a unique set of their physical properties in combination with the possibility of controlling them in very wide ranges by varying the deposition parameters. The most useful of these properties are the high adhesion of the films to different substrates, high hardness (15–28 GPa) [4], low friction coefficient (~0.1) [5, 6], and low roughness (≤ 1 nm) [7]. In addition, a valuable feature of the fabrication technique is the possibility of obtaining a specified resistivity in the range of 10^{13}–10^{-4} Ω cm [3].

All aforesaid makes the DLN films promising for use in various fields of science and technology, including tribology (both on earth and in space), IR optics, radio engineering, micro- and nanoelectronics, and medicine. Most properties of the DLN films are structurally sensitive and have pronounced percolation dependences [8] on the nanophase concentration. The behavior of the dependences is affected by the structure, morphology, and character of the nanophase distribution in the matrix bulk. The use of DLN films calls for intense and detailed study of the dependences of their properties on the three latter parameters. Here, the main problem is the strict differentiation of the available methods for studying the volume and morphology of an object of study. In particular, X-ray reflectometry yields data on film layers with characteristic thicknesses of no more than 100 nm and areas of several square centimeters. In electron microscopy, the object thickness may be of the same order of magnitude, but the area is only few square microns. Scanning probe microscopy has intermediate capabilities, but is a purely surface technique. A comparison of the data obtained using these three techniques may lead, upon their accumulation, to the synergy and significantly improve the knowledge about the investigated films, which is an urgent problem.

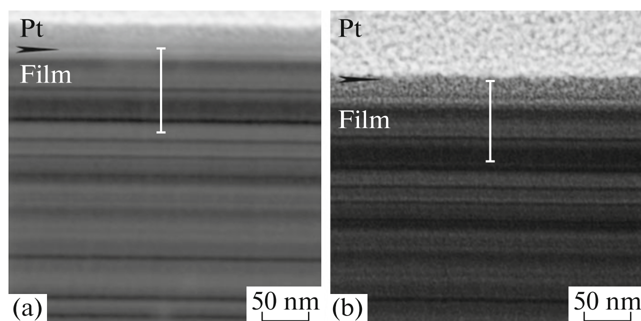

Fig. 1. TEM images of the surface structure of DLN films with vanadium contents of (a) 12 and (b) 17 at %. Vertical lines show the domains of definition of brightness profiles (the line length is 80 nm).

TECHNIQUE FOR FABRICATING VANADIUM-DOPED DLN FILMS

Vanadium-doped DLN films were formed by deposition in a vacuum chamber with two different precursor sources: an original plasmatron and a conventional magnetron [2]. The chamber was a cylinder (∅ = 70 cm and $L = 50$ cm) with a horizontal axis of rotation, with the ends closed by flat round caps. The sources were located on a horizontal diameter of one of the caps on the opposite sides from the center and at the same distance (15 cm) from it. The substrate holder was located on the opposite cap and had a round shape (∅10–60 cm), with an axis of rotation coinciding with the chamber axis. The speed of rotation of the substrate holder was 0–10 rpm. The required vacuum level was provided by backing and diffusion pumps. The films for study were grown by simultaneous deposition of a silicon-carbide matrix from PMPS vapor plasma and magnetron sputtering of a vanadium target in an argon atmosphere under a partial pressure of 8×10^{-4} Torr. The initial substance for the matrix was PMPS 2.5L, which is a liquid compound with a formula $(CH_3)_3SiO(CH_3C_6H_5SiO)_3Si(CH_3)_3$ and a boiling point of 130–140°C. PMPS molecules in plasma dissociate (under the action of accelerated electron flow from the tungsten cathode of the plasmatron) along weak bonds with a release of hydrogen ions and CH_x radicals, carbon radicals associate with the formation of diamond-like sp^3 carbon bonds, and hydrogen ions associate with silicon bonds [9]. PMPS was also used as a working liquid of the diffusion pump. This feature, i.e., the same composition of the diffusion pump vapor and the plasma-forming substance vapor, allows one to do without nitrogen traps. The second feature of the technique applied is a peculiar way of introducing the plasma-forming substance into the chamber. PMPS was fed into the reactor through a standard needle leak valve due to the pressure difference between the chamber and environment. In the plasmatron, the liquid enters its front part (made of porous corundum ceramics), located in the chamber near the tungsten cathode. The cathode temperature is higher than 2000°C, and the cathode potential is shifted by 100–200 V below the ground potential. Due to the effect of thermal radiation from the cathode, the ceramics is heated above 300°C and PMPS passes to the gaseous state and enters the chamber as a directed flow through the pores in the ceramics. The high-intensity thermionic emission of the cathode converts the vapor into a plasma. A high-frequency (1.7 MHz) potential with an amplitude in the range from 100 to 400 V was applied to the substrate holder.

To estimate the time necessary to form films of desired thickness, we applied the calibration curves obtained in tests. Two film samples with vanadium contents of 12 and 17 at % were investigated.

METHODS AND RESULTS

Electron Microscopy

The film structure was investigated using transmission electron microscopy (TEM) on a FEI Tecnai Osiris microscope at an accelerating voltage of 200 kV. Figure 1 shows cross-sectional TEM images of the DLN films. During sample preparation, the film surface was coated with a protective Pt layer with a thickness of about 1 μm. According to the TEM data, the film thicknesses are 3.8 μm (12 at % V) and 3.75 μm (17 at % V). The images demonstrate that the films have a layered structure without visible defects and discontinuities. The layered structure is caused by the chemical inhomogeneity of the films, which results in the release of vanadium carbide (VC) nanocrystals [10].

X-Ray Reflectometry

An X-ray diffractometer with a mobile tube–detector system [11] makes it possible to measure the intensity of both the reflected X-ray radiation and the radiation scattered from the sample surface. The X-ray optical path of the diffractometer includes a three-slit collimator, a single-reflection Si(111) crystal monochromator, and vacuum paths for reducing the radiation absorption in air. A sample was mounted on an alignment table, with surface oriented parallel to the incident beam propagation direction (beam axis). In further measurements, the sample remained fixed, while the source and detector were rotated around it at specified angles. Solving the inverse X-ray reflectometry problem, one can reconstruct the distribution of the real part of the permittivity (proportional to the volume electron concentration in the material) in the direction perpendicular to the surface from the angular dependence of the X-ray reflecivity (Fig. 2). To this end, a model-independent approach was used, which does not require any a priori information about the internal structure of the object under study [12].

To compare the results obtained by solving the inverse X-ray reflectometry problem, we used electron

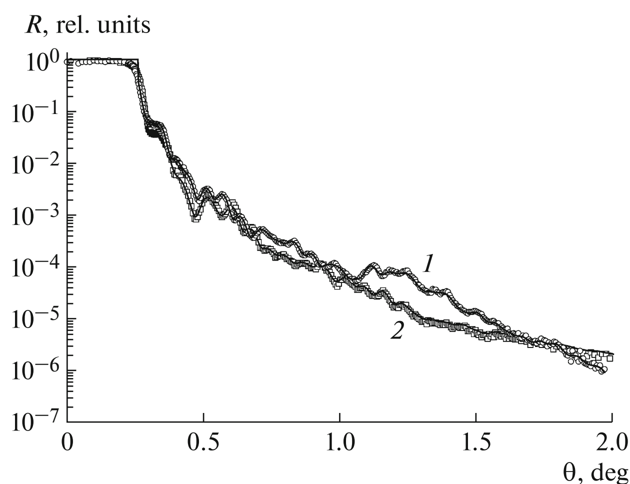

Fig. 2. Angular dependences of the experimental (symbols) and simulated (lines) reflectivities for the DLN films with vanadium contents of (*1*) 12 and (*2*) 17 at %.

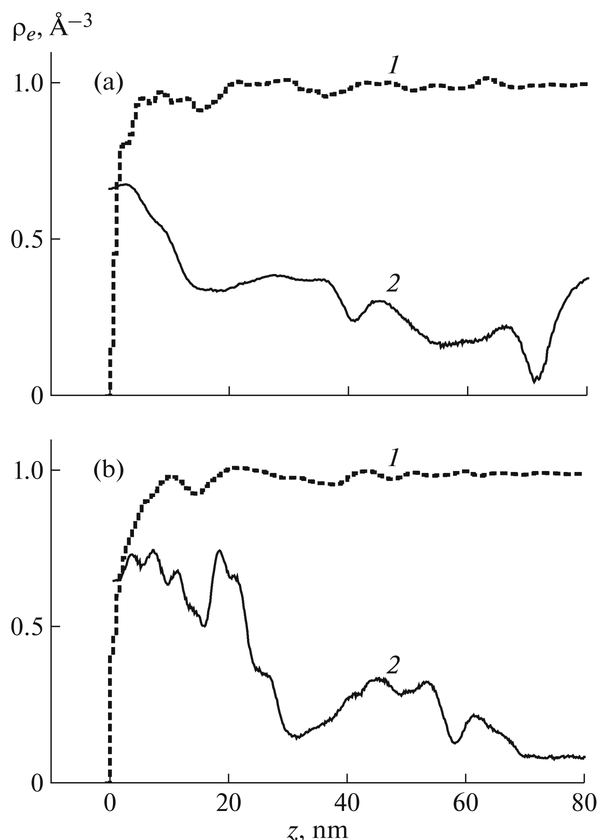

Fig. 3. (*1*) X-ray reflectometry electron density profiles and (*2*) TEM brightness profiles averaged over the lateral plane in the range of 20 nm for the DLN films with vanadium contents of (a) 12 and (b) 17 at %.

microscopy images to calculate the brightness profile along the corresponding specified direction and on a comparable scale (vertical lines in Fig. 1). The calculation was performed with averaging the brightness data in the lateral plane over a 20-nm-wide area. The results obtained for the samples with vanadium contents of 12 and 17 at % are compared in Fig. 3.

The X-ray data were averaged over an area corresponding to the surface area exposed to the X-ray beam (~50 mm^2), which significantly exceeding the TEM measurement area. Hence, the coincidence of the positions of some main peaks indicates that the layered structure of the film is retained to a certain extent on the macroscale. The difference in the other features of the curves is probably due to some nonuniformity of the layer thickness in the film, which is caused by the change in the distance to the sputtering sources of film materials at different portions along the surface, as well as the ambiguity in specifying the position of the "outer surface" of the structure in the TEM images, which is caused by deposition of protective Pt layer on it.

To estimate the statistical nonuniformity of the layer parameters in the direction perpendicular to the surface, the frequency spectrum function was calculated (using the Fourier cosine transform) for the obtained distributions of electron concentration and brightness (Fig. 4)

$$PSD_{1D}(\nu) = 4\int C(z)\cos(2\pi\nu z)dz,$$

where ν is the spatial frequency, z is the coordinate in the direction perpendicular to the surface, and $C(z)$ is the autocorrelation function.

This spectral representation of the statistical spatial characteristics of physical objects was used previously to describe the roughness parameters of supersmooth surfaces. Some studies demonstrated its feasibility when comparing the data obtained using techniques based on different physical principles [13, 14].

It is worth noting that, in contrast to the calculated power spectral density of roughness heights, where the experimental data of all types are ultimately related to the surface profile, the image brightness and the real part of the permittivity agree only qualitatively in our case, which excludes the possibility of direct comparison of the obtained amplitude curves. In the frequency characteristics, where the spatial frequency is inverse to the period along the coordinate that used in calculation, one can observe some regularities, which manifest themselves as coinciding peaks, corresponding to periods of 3.8 and 7.4 nm. These values can be used to characterize the averaged layer thicknesses in the film structures and their coincidence is indicative of partial but significant preservation of the periodicity of the spatial characteristics of the structure on the macroscale.

Atomic Force Microscopy

Atomic force microscopy (AFM) measurements were performed on an NT-MDT NTEGRA Prima

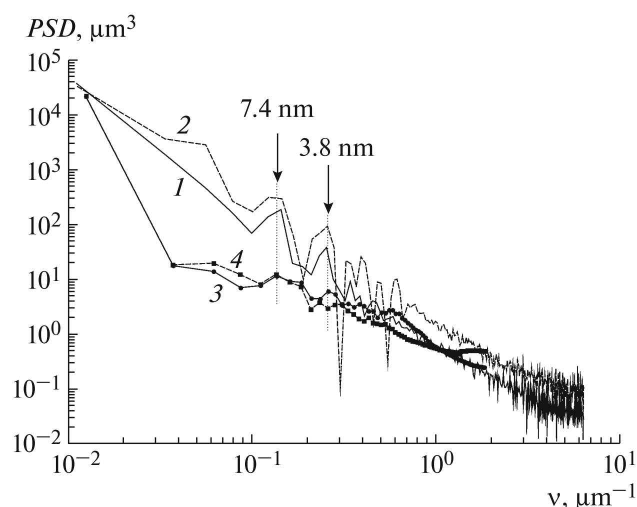

Fig. 4. Frequency spectra of the (*1*, *2*) TEM brightness profiles and (*3*, *4*) X-ray reflectometry electron density profiles.

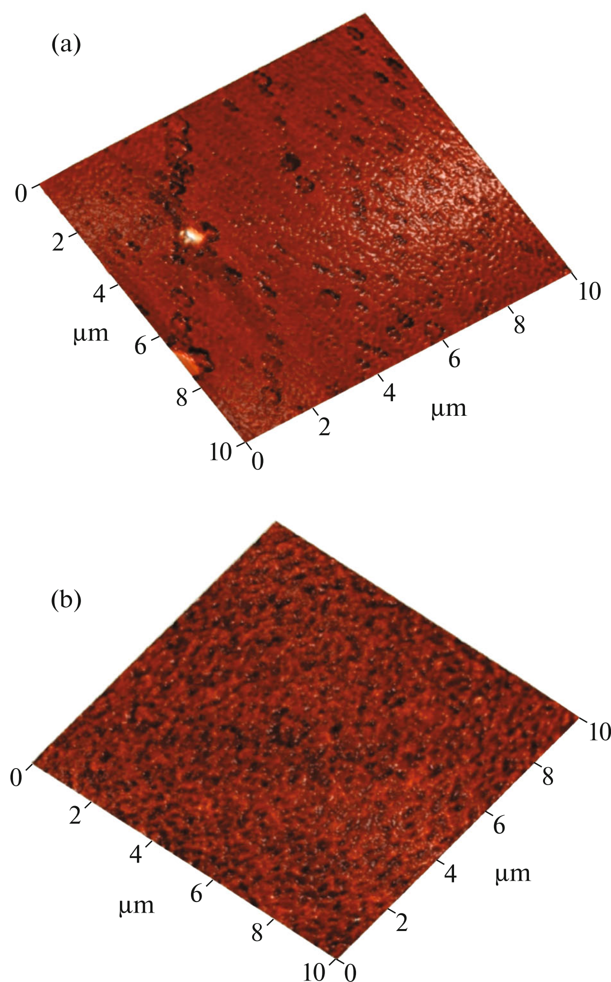

Fig. 5. AFM surface images of DLN films with vanadium contents of (a) 12 and (b) 17 at %.

scanning probe microscope in the semi-contact mode. Scanning of each sample was performed at two points: point *1* at the center of the plate and point *2* at a distance of 3 mm from the plate edge. The topography data were processed using the Nova software (supplied with the microscope). The AFM images are presented in Fig. 5.

The sample with a vanadium content of 12 at % is characterized by a large root-mean-square height of the surface roughness: about 1.7–2.3 nm. The surface contains craters with a lateral size up to 100 nm and a depth up to 10 nm, which have a high distribution density over the surface.

The measurements on the sample with a vanadium content of 17 at % showed its low roughness with a root-mean-square value of 0.2–0.3 nm, which is characterized by the high surface uniformity of the parameters. The differences in the roughness values measured at points *1* and *2* were no more than 3–5%; therefore, the data taken at one point are presented. A chaotic distribution of protrusions and valleys is observed for both samples. No static charge was detected in them.

CONCLUSIONS

The use of an integrated approach combining a direct method for determining the film structure in the nanometer range (transmission electron microscopy) and a non-destructive method providing averaged information about the coating thicknesses in a wide range in the lateral direction (X-ray reflectometry) made it possible to establish that the strip-layered structure, characteristic of vanadium-doped silicon nanocomposite carbon films, is retained on average over the entire sample surface. A statistical approach was proposed to describe the parameters of the spatial structure of multilayer films and characterize quantitatively the degree of disordering of constituent layer thicknesses. The conclusion that the layered film structure is preserved as a whole over large areas and depths is important, because it indicates that the technology is reproducible and, therefore, can be applied in practice. A significant decrease in the root-mean-square surface roughness of the DLN film with an increase in the vanadium content from 12 to 17 at % was established. At first glance, this circumstance seems paradoxical, because one could expect an increase in the surface roughness with an increase in the dopant (vanadium) concentration. However, similar results were obtained on samples of the same composition and investigated using the same method but on another atomic force microscope. Further investigations are necessary to explain this phenomenon.

FUNDING

The study was supported by the Russian Science Foundation, project no. 15-12-00039, in the part concerning the synthesis of vanadium-doped DLN films; the Ministry of Science and Higher Education of the Russian Federation within a state assignment, project no. 16.9350.2017/8.9, in the part concerning the structural studies of the films; and the Ministry of Science and Higher Education of the Russian Federation within a state assignment for the Federal Research Center "Crystallography and Photonics" of the Russian Academy of Sciences in the part concerning the development of the technique for comparing X-ray diffraction and electron microscopy data.

REFERENCES

1. Š. Meškinis and A. Tamulevičienė, Mater. Sci. (medžiagotyra) **17** (4), 358 (2011).
2. M. L. Shupegin, Zavod. Lab. Diagn. Mater. **79** (2), 28 (2013).
3. V. F. Dorfman, Thin Solid Films **212**, 267 (1992).
4. E. V. Zavedeev, O. S. Zilova, A. D. Barinov, et al., Diamond Relat. Mater. **74**, 45 (2017).
5. T. W. Scharf, J. A. Ohlhausen, D. R. Tallant, et al., J. Appl. Phys. **101**, 063521 (2007).
6. S. M. Pimenov, E. V. Zavedeev, N. R. Arutyunyan, et al., J. Appl. Phys. **122**, 145301 (2017).
7. E. V. Zavedeev, B. Jaeggi, J. Zuercher, et al., Wear **416–417**, 1 (2018).
8. V. F. Dorfman, Thin Solid Films **330**, 76 (1998).
9. A. I. Belogorokhov, A. N. Dodonov, M. D. Malinkovich, et al., Mater. Elektron. Tekh., No. 1, 69 (2007).
10. O. M. Zhigalina, D. N. Khmelenin, S. M. Pimenov, et al., Crystallogr. Rep. **63** (5), 796 (2018).
11. V. E. Asadchikov, V. G. Babak, A. V. Buzmakov, et al., Prib. Tekh. Eksp., No. 3, 99 (2005).
12. I. V. Kozhevnikov, Nucl. Instrum. Methods Phys. Res. A **508**, 519 (2003).
13. M. L. Zanaveskin, I. S. Zanaveskina, B. S. Roshchin, et al., Vestn. Mosk. Univ., Ser. 3: Fiz., Astron., No. 3, 80 (2006).
14. V. E. Asadchikov, I. V. Kozhevnikov, B. S. Roshchin, et al., Mir Izmer., No. 7, 22 (2012).

Translated by E. Bondareva